Computer Vision Techniques Applied to Space Object Detect, Track, ID, and Characterize

Brien Flewelling, PhD
Air Force Research Laboratory Kirtland AFB, NM

Brad Sease
Virginia Polytechnic Institute and State University, Blacksburg, VA

ABSTRACT

Space-based object detection and tracking represents a fundamental step necessary for detailed analysis of space objects. Initial observations of a resident space object (RSO) may result from careful sensor tasking to observe an object with well understood dynamics, or measurements-of-opportunity on an object with poorly understood dynamics. Dim and eccentric objects present a particular challenge which requires more dynamic use of imaging systems. As a result of more stressing data acquisition strategies, advanced techniques for the accurate processing of both point and streaking sources are needed. This paper will focus on two key methods in computer vision used to determine interest points within imagery. The Harris Corner method and the method of Phase Congruency can be used to effectively extract static and streaking point sources, and to indicate when apparent motion is present within an observation. The geometric inferences which can be made from the resulting detections will be discussed, including a method to evaluate the localization uncertainty of the extracted detections which is based on the computation of the Hessian of the detector response. Finally, a technique which exploits the additional information found in detected streak endpoints to provide a better centroid in the presence of curved star streaks is explained and additional applications for the presented techniques are discussed.

1. INTRODUCTION

There is much room for methods of computer vision and image processing to increase the utility of existing space object tracking sensors. Space object tracking imagery contains rich information, not all of which is being exploited effectively. As a result of image processing algorithms being written to handle a specific type of acquisition strategy, sensor sites may be limited in the types of observations and resulting data products which may be reported from the data they collect. There have been several papers [1,2] which have discussed front end image processing architectures which process imagery collected in sidereal stare [1] and rate track [2] modes. What is desired is a general image processing architecture capable of effectively analyzing imagery collected over any motion achievable by the optical system. To this end computer vision techniques may be used to infer general rotational motion of an optical system with respect to a star field. This paper seeks to motivate the use of additional image features to perform online geometric analysis of detected signals, enabling when possible more than just inferences of detected angles, angle rates, and brightness of objects determined by centroids.

The geometric analysis introduced in this paper will be shown to be effective in the presence of stray light, or non-uniform scene energy, as well as enable on the fly determination of sensor rotational motion and discrimination of resident space objects. The proposed processing is motivated by the recent proliferation of small telescope technology which makes new sensor architectures possible which may operate in a dedicated tracking and characterization mode where imagery could be taken at video rates. The rest of this paper is organized as follows: section 2 will describe two methods of signal extracted not based on intensity thresholds but on characteristics of locally compact signals. Section 3 will discuss a method for the determination of centroid and endpoint uncertainty using the Hessian of the detector output. Section 4 presents an approach to determining the rotation axis and rate of a slewing imaging system which may be used to simultaneously identify candidate RSO's for subsequent tracking and characterization. Section 5 presents a method for mapping image data to a new representation in polar coordinates centered on the determined axis of rotation. In this representation, a match filter can be easily derived for the identification and extraction of streaking star signals which may be both dim and curved in the original image.

2. SIGNAL EXTRACTION BASED ON LOCAL CURVATURE AND LOCAL ENERGY

There is a large body of work dedicated to the extraction of signals from imagery for the purposes of space object tracking. A key assumption in many methods is that the segmented pixels associated with a given object may be "centroided" and the resulting vector will be the direction to the space object. For unresolved objects the center of brightness, or intensity weighed centroid is used to derive the vector direction to stars and RSOs. As objects become partially resolved or fully resolved however, the center of brightness may no longer represent the actual direction to the center of mass of the space object. Thus, multiple methods of the extraction of information of detections can be used to infer characteristics of observed objects. Two methods will be presented here. One method is based purely on image intensity gradients and is considered a standard in feature point extraction for object tracking in computer vision. The second method is based on frequency domain arguments and has many desirable behaviors for processing space imagery. In the case of perfect observation of a static source, centroids based on intensity, local curvature, and local energy reside in the same place. When these detection locations are not in close agreement, it can be used as an indicator of non-ideal observation conditions which may cause a need for deeper analysis of the detection.

An elegant approach to corner detection was presented in 1988 by Harris and Stephens [3]. In this work they showed that typical local minimum of the auto-correlation function required of a corner or a "good point to track" is easily determined by the image gradients. Instead of comparing windows over a predefined neighborhood about an image pixel, they define the structure tensor over a point neighborhood and introduced a Gaussian weighting. By evaluating the eigenvalues of the structure tensor one may classify pixels as belonging to a local edge response, corner response, or bland region. For all participating pixel members of a Gaussian weighted neighborhood, the weighted sum of squared differences is given by:

$$SSD(x,y) = \sum_i \sum_j w(i,j)(I(x+j, y+i) - I(i,j))^2 \tag{1}$$

Here (i; j) are the vertical and horizontal displacement indices of the pixel neighbors. The weighting function w(i, j) is a Gaussian weighting function chosen to match the size of the pixel neighborhood. The displaced pixel I(x + j, y + i) intensity can be approximated by using the Taylor Series expansion as:

$$I(x+j, y+i) - I(i,j)) = I(i,j) + I_x(i,j)x + I_y(i,j)y \tag{2}$$

By substitution we obtain:

$$SSD(x,y) = \sum_i \sum_j w(i,j)(I_x(i,j)x + I_y(i,j)y)^2 \tag{3}$$

The expression above is a weighted quadratic function of the image partial derivatives and (x, y) displacements of the pixel neighbors. This can be represented more generally in matrix-vector form by:

$$SSD(x,y) = \begin{bmatrix} x & y \end{bmatrix} A \begin{bmatrix} x & y \end{bmatrix}^T \tag{4}$$

The eigenvalues of the matrix A provide the proportions of the principle curvatures of the local autocorrelation function. Simply put these values provide a direct means of evaluating the local curvature of image data. For a corner response, both eigenvalues should be high; this implies a direct relationship to the minimum eigenvalue detection method also common in feature extraction. A pixel residing on an edge response will have only one large eigenvalue. Finally a pixel located in a bland region will have small eigenvalues. The Harris response function was developed to quickly compare the eigenvalues of the structure tensor and determine the degree to which the data was curved and therefore represented a corner. It is given by:

$$R = det(A) - kTr^2(A) = \alpha\beta - k(\alpha + \beta) \quad (5)$$

Here, k is an empirically determined constant used to scale the relative size of the eigenvalue sum compared to the product of the eigenvalues. By applying a threshold to the response function instead of directly computing and comparing the eigenvalues, corner feature strength can be determined without having to compute the more costly square roots involved in the eigenvalue decomposition. This approach works for images of any resolution, and has seen wide application. The result of applying the Harris corner detector to an image of a star field is shown in figure 1. Notice how both the rate-tracked RSOs and the endpoints of the streaking stars are highlighted in the cornerness response. The addition of endpoint information to standard detection or centroiding enables the estimation of additional parameters of the observation. In this case the right ascension and declination rates of the observation can be measured by determining the streak lengths of the stars as well as the ID's for each star. An undesirable trait of Harris corner localization results from its dependence on the computation of image gradients. Often it is necessary to combine a smoothing operation with the computation of spatial gradients within an image. This is especially required in noisy imagery. The result is that the computed peaks can be slightly biased at streak endpoints where the signal is not symmetric. Care must also be taken to ensure that the smoothing kernel scale is carefully selected. Note in figure 1 that the RSO signals are not centrally located since the kernel was selected to find endpoints of the streaking stars. For imagery where significant variation in star and RSO signal scales can be expected, a multi-scale Harris approach is required. While this method is useful in determining additional features of detected objects, it is not immediately amenable to direct extraction of the star streaks and RSO signals. A better method for direct extraction is to perform segmentation based on the local energy model.

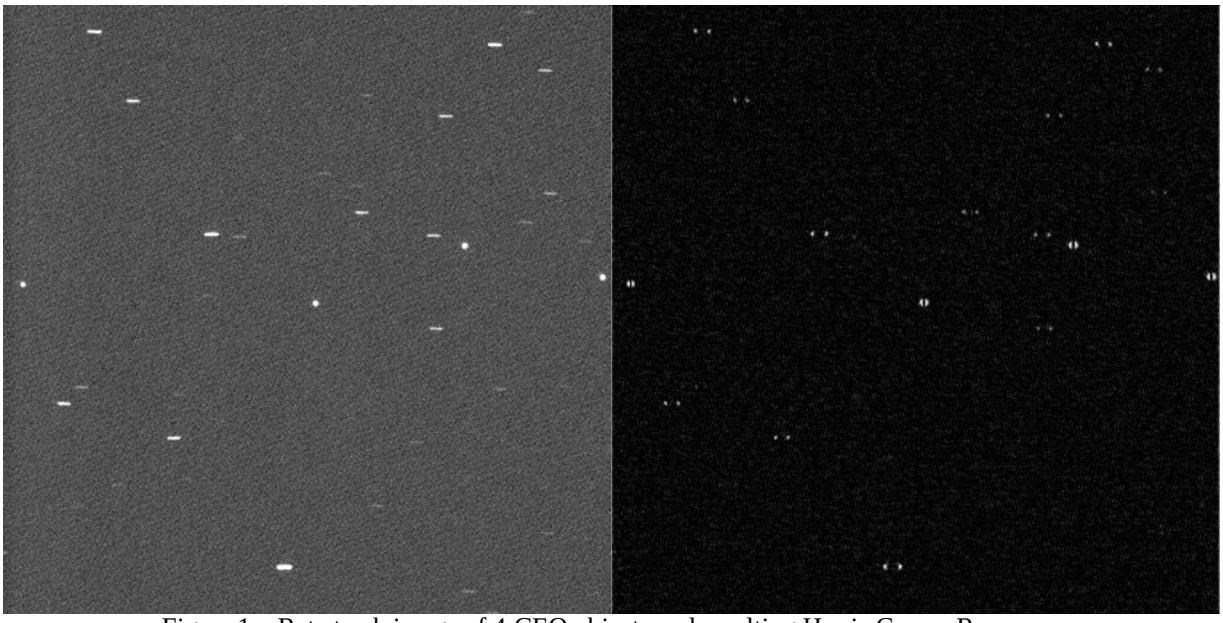

Figure 1 – Rate track image of 4 GEO objects and resulting Harris Corner Response

The Phase Congruency model for feature detection [4] is not based on image gradients, but on local Fourier components of a signal. If one were to represent a location in an image by a local Fourier series expansion, that location would be considered perceptible if multiple local Fourier components were in phase. Phase Congruency at any angle indicates a perceptible feature, and the angle at which these components are in phase can be used to characterize feature type. It would be interesting to investigate the use of the angle of congruency as a method for characterization of RSO's but that analysis is left for future work. This characteristic of image data was first analyzed as part of the development of the local energy model which has been used by Morrone [5] while attempting to explain many psychophysical effects of human perception. The practical use of this model for the detection of edges and corners in imagery was introduced by Kovesi [4]. In his work he explains that one may interpret the phase congruency in any location of the image as the ratio of the radial extent of the path taken by adding the complex valued vectors of each Fourier component in the phase plane head to tail, to the overall distance traveled by adding the vectors.

$$PC(x) = \frac{|E(x)|}{\sum_n A_n(x)} \tag{6}$$

The resulting value is bounded between 0 and 1 which makes interpreting the output of applying Phase Congruency to and image convenient. Additionally it is straight forward to apply the process to a noisy image from a given sensor and determine a threshold value which will produce a desired level of false positives. Figure 2 shows the concept of local frequency components being in phase in the vicinity of a feature as well as a visualization of the geometric interpretation just described.

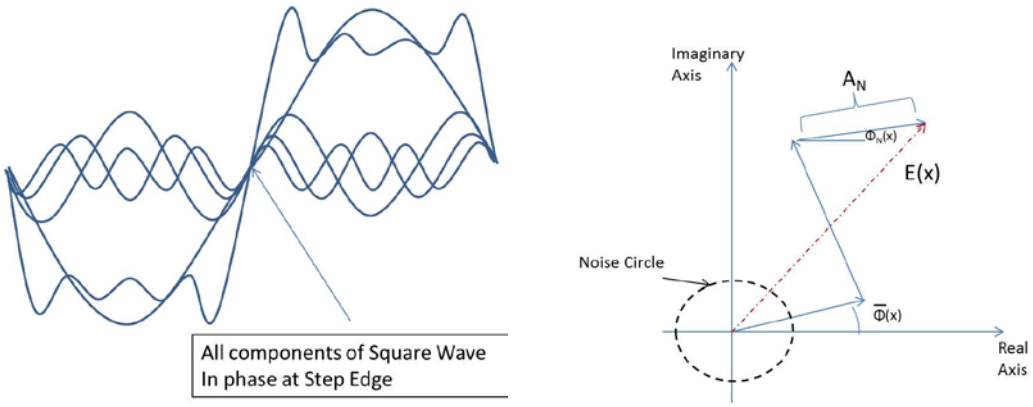

Figure 2 (left) Multiple Fourier Components of a periodic signal in phase at the step edge, (right) Fourier components plotted tip to tail in the polar diagram

In very much the same way as corners and edges were determined using the Harris approach, moments may be taken of the Phase Congruency measure and used to indicate the same structure. One may build the matrix:

$$A = \begin{bmatrix} PC_x^2 & PC_x PC_y \\ PC_y PC_x & PC_y^2 \end{bmatrix} \tag{7}$$

In this case the minimum and maximum singular values correspond to the minimum and maximum moments of Phase Congruency. In contrast to the edge and corner responses of the Harris method, or in edge and corner detections in general, the corner map generated by this algorithm is a strict subset of the edge map. This means that extracted edges will have corners associated with their endpoints. This has particular use in this application because it makes the output immediately capable of direct extraction of static or trailing point sources. The correct extraction of stars and RSO's can be made invariant to sensor motion which is very desirable. Figure 3 shows the results of applying the Phase Congruency algorithm to the same image as was used in the Harris detector case. Here a threshold is set on the minimum moment of Phase Congruency in order to distinguish signal from noise. Notice that the resulting segmentation mask accurate identifies pixels belonging to both the rate tracked RSOs and the streaking stars. Additionally the endpoints of the streaking stars stand out as additional corners, an effect shared by the Harris detector. In contrast however one may use this method to perform initial signal extraction, and subsequent geometric analysis, thus providing not only the center of brightness defined by the intensity of the segmented pixels but the center of the phase congruency weighting and any other additional peaks which may be important.

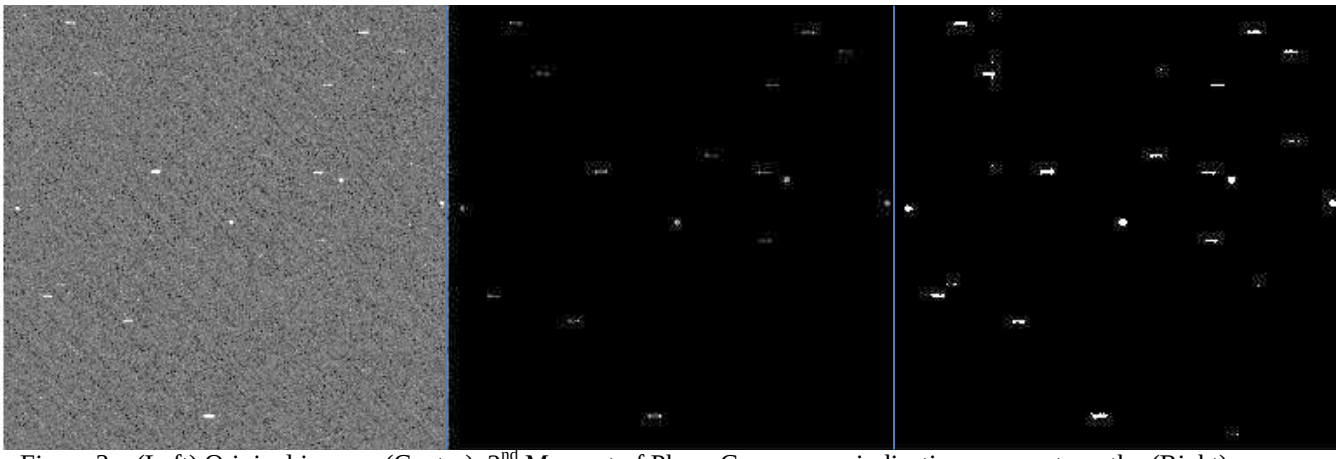

Figure 3 – (Left) Original image. (Center) 2nd Moment of Phase Congruency indicating corner strength. (Right) Resulting segmentation mask derived by thresholding the 2nd Moment value.

Figure 4 demonstrates the robustness of this method to stray light. Since the value being thresholded is a dimensionless quantity invariant to image contrast, the output performance of the method is identical even though a significant ramp has been added to the background noise of the signal. This effect is very desirable for developing an image processing engine that is capable of handling varying background noise and stray light. In the next sections, we will demonstrate how the output of these methods can be used to define detection uncertainty and to infer both sensor and object motion from imagery alone.

.

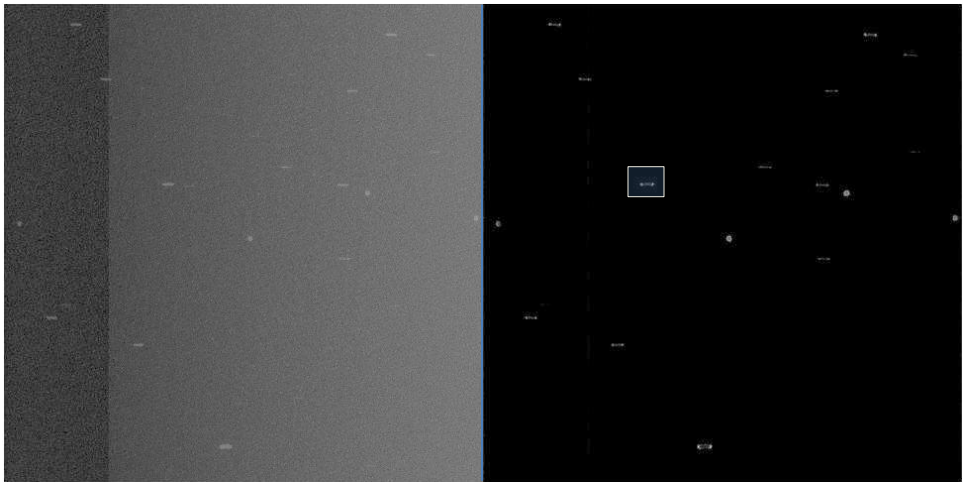

Figure 4 – (Left) Original image with addtion of discontinuous non-uniform noise floor. (Right) Result of Phase Congruency computation. The structure of the output is invariant to the presence of the background variation.

3. CENTROID AND ENDPOINT UNCERTAINTY DETERMINATION

The direct computation of uncertainty in point based features is well known in computer vision. While many methods which use principle component analysis (PCA) or information contained in the eigenvalues computed from the positions and values of segmented pixels exist, a direct relationship between the local Hessian of the detector response function and the localization uncertainty has been derived and effectively used for many feature extraction and tracking applications [6]. The hessian is the matrix of second order partial derivatives which may be computed for every pixel of any image. For example localization uncertainty is expressed as the inverse of the local hessian matrix of the Phase Congruency response:

$$H[PC(x*, y*)] = \frac{\partial PC(x,y)}{\partial l \partial l'} \Big|_{x=x*, y=y*} = \Sigma^{-1}_{PC(x,y)} \quad (8)$$

Here, l and l' may take both values x and y in order to fill out the four partial derivatives which comprise the matrix. Figure 5 demonstrates the computation of localization uncertainty at every pixel of the Phase Congruency algorithm response computed in the vicinity of a streak (highlighted by the box in figure 4). The minimum localization uncertainty coincides with the peak values detected at the streak endpoints.

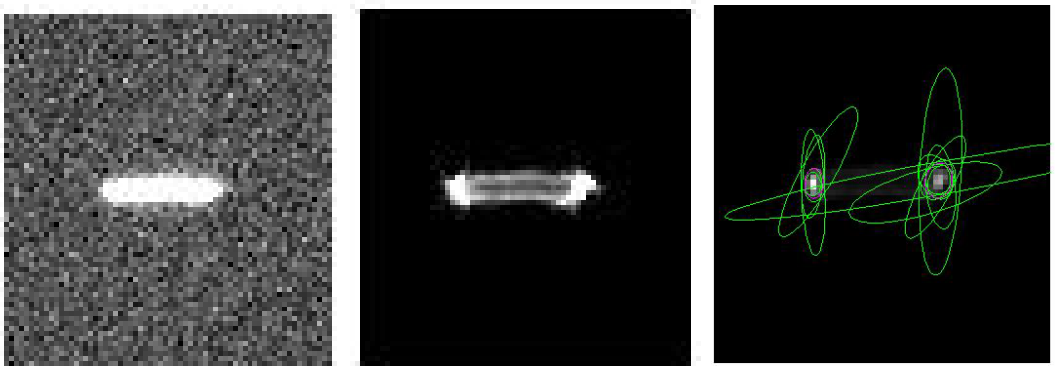

Figure 5 – (Left) Local neighborhood of Original image. (Center) Local Phase Congruency Computation. (Right) Uncertainty calculated for each pixel of sufficient response. Minimum covariance is located at the detection peaks.

In stark contrast, one may use a match filter which assumes a-priori knowledge and evaluate the a-posteriori localization uncertainty by computing the Hessian of the match filter response as shown in figure 6.

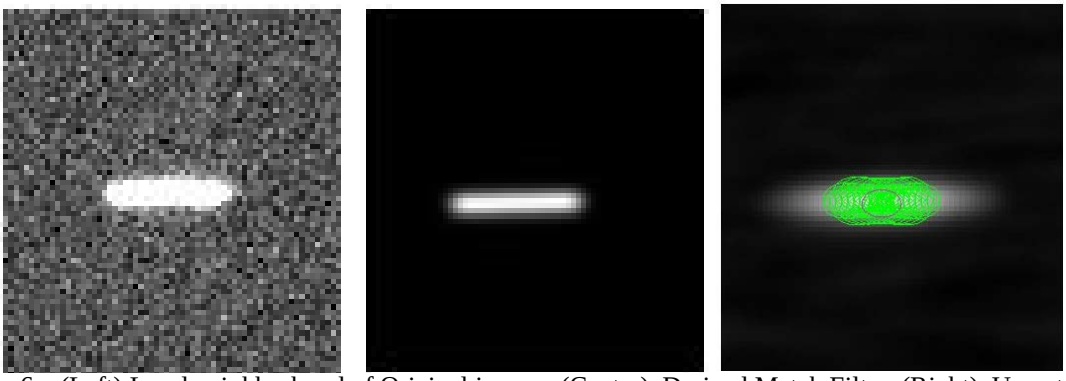

Figure 6 – (Left) Local neighborhood of Original image. (Center) Derived Match Filter (Right) Uncertainty calculated for each pixel of sufficient response. Minimum covariance is located at the detection peaks.

Without prior information detection uncertainty and knowledge of the signal geometry in an image is coupled. An iterative procedure can be easily designed which progresses from zero *a-priori* detection, to maximum *a-posteriori* signal extraction by minimizing the localization uncertainty and maximizing the knowledge of the observed trajectory within the frame. The next sections will show how this information can be used to effectively discriminate RSOs from stars, and to determine important parameters describing an image taken from a slewing platform.

4. ONLINE DETERMINATION OF FIELD ROTATION AND DISCRIMINATION OF RSO's

With a set of endpoints for all signals detected within an image, we are able to infer additional information about the motion of the sensor as well as the particular behavior of individual signals. To achieve this, we must first group the endpoints according to occurrence in time. Note that there is an ambiguity in which endpoints occurred at the initial

time and which correspond to the final time, however we are able to determine which endpoints likely occurred simultaneously. This solution takes a geometric approach in the image plane to determine the probable intersection of the axis of rotation with the image plane, hereafter referred to as the center of rotation.

Assuming that each signal corresponds only two endpoints, we begin by computing the midpoint of the endpoint pair, $(x_{i,c}, y_{i,c})$, where $i = 1,2,\dots,N$ designates the signal index. With this point and the slope of the line connecting the endpoint pair, m_i, we are able to write the equation of perpendicular line passing through the midpoint as

$$y - y_{i,c} = \frac{1}{m_i}(x - x_{i,c}) \tag{9}$$

Rearranging,

$$y - \frac{1}{m_i}x = -\frac{1}{m_i}x_{i,c} + y_{i,c} \tag{10}$$

The intersection of the perpendicular lines for each streak corresponds to the location of the center of rotation. We are able to build a least-squares problem of the form $AX = b$,

$$\begin{pmatrix} 1 - \frac{1}{m_1} \\ 1 - \frac{1}{m_2} \\ \vdots \\ 1 - \frac{1}{m_N} \end{pmatrix} X = \begin{bmatrix} -\frac{1}{m_1}x_{1,c} + y_{1,c} \\ -\frac{1}{m_2}x_{2,c} + y_{2,c} \\ \vdots \\ -\frac{1}{m_N}x_{N,c} + y_{N,c} \end{bmatrix} \tag{11}$$

Where $X \in R^2$ denotes the center of rotation. The least-squares estimate of the center of rotation, then, is given by

$$\hat{X} = (A^T A)^{-1} A^T b \tag{12}$$

To correctly group simultaneously occurring endpoints, we compute the vector from each midpoint to each of its corresponding endpoints and consider the vector from the center of rotation to each midpoint, as seen in Figure 7.

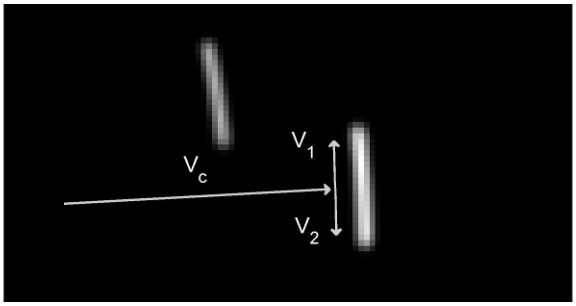

Figure 7 – Vector cross product operation for endpoint grouping

The correct endpoint grouping follows from a cross product operation between V_c and the endpoint vectors, V_1 and V_2, for each streak. A sign difference in third component of the result is an indicator of endpoint grouping, i.e.

$$[V_c \times V_1]_3 = -[V_c \times V_2]_3 \tag{13}$$

Note that in order for the cross-product to be defined, all three vectors must be augmented with an arbitrary third component. For scenarios where the streaks are nearly straight, the term $A^T A$ approaches singularity. In this case,

however, the grouping of endpoints is fairly trivial. Note that any center of rotation estimate beyond the bounds of the image and along the perpendicular line of any streak will provide the correct endpoint groupings with the vector cross-product procedure.

The correct endpoint grouping now allows an estimate of the field rotation from a single frame. By computing the body-fixed unit vector corresponding to each endpoint, we are able to formulate Wahba's problem,

$$L_W(\hat{A}) = \frac{1}{2}\sum_{i=1}^{N} \alpha_i \left\| b_i - \hat{A} r_i \right\|^2 \tag{14}$$

where b_i and r_i are two sets of unit vectors, $\hat{A}$ describes the rotation between them, and α_i is a set of weightings [7]. Many solutions of Wahba's problem exist which will provide an estimate of the rotation between the two endpoint groups [8, 9]. This solution additionally provides a method of detecting RSOs. Computing the residuals of the rotation estimate as

$$e_i = \left\| b_i - \hat{A} r_i \right\|^2 \tag{15}$$

yields an indicator of non-star behavior. Note that this works under the assumption that the field contains mostly star streaks and only a small number of RSOs. In scenarios with closely-spaced objects and a small field of view, the rotational estimate may become biased by the RSO detections such that it becomes unreliable.

5. STREAK PROCESSING IN POLAR COORDINATES

Knowledge of the sensor rotation allows us to perform a more thorough analysis of the imagery to discover additional signals. In general, it is possible to extract dim signals from an image with knowledge of the appearance of the signal uncorrupted by noise. This template matching procedure is referred to as a matched filter [10]. From the reference frame of a rotating sensor, however, characterization of the expected size and shape of a star signal becomes more complicated. In the case of Figure 8, we see that the size and shape of a star streak is dependent on its location within the image. One could perform and adaptive matching process, wherein the algorithm generates the expected signal for each location in the image, however this would be a computationally intensive algorithm.

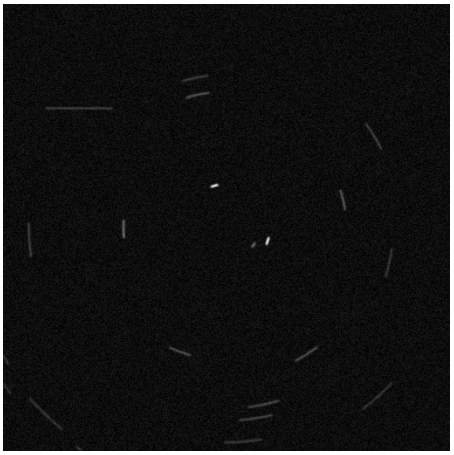

Figure 8 – Streaked star image with an RSO

Alternatively, we are able to utilize the center of rotation estimate, derived in the previous section, to simplify the pattern matching procedure. By re-sampling the image in polar coordinates about the center of rotation, we are able to produce an image where star signals are equal length, and that length corresponds directly to the angle of rotation

of the sensor. We define a polar coordinate system with the center of rotation, X, as the origin. The relation between the (x, y) image coordinates and (r, θ) coordinates is

$$x = rcos(\theta) + X_1$$
$$y = rsin\theta + X_2 \quad (16)$$

Thus a grid of (r, θ) coordinates can be converted to (x, y) coordinates, enabling the user to re-sample the original image in the polar coordinate frame. The image from figure 8 is seen again in figure 9, re-sampled in the polar coordinate frame about the center of rotation. Note that interpolated values of regions beyond the image boundaries are undefined. These should be indicated as such and removed from consideration in future processing. Here, out-of-bounds regions are marked as NaN (not a number), and can be seen in the lower portion of the image as dark areas.

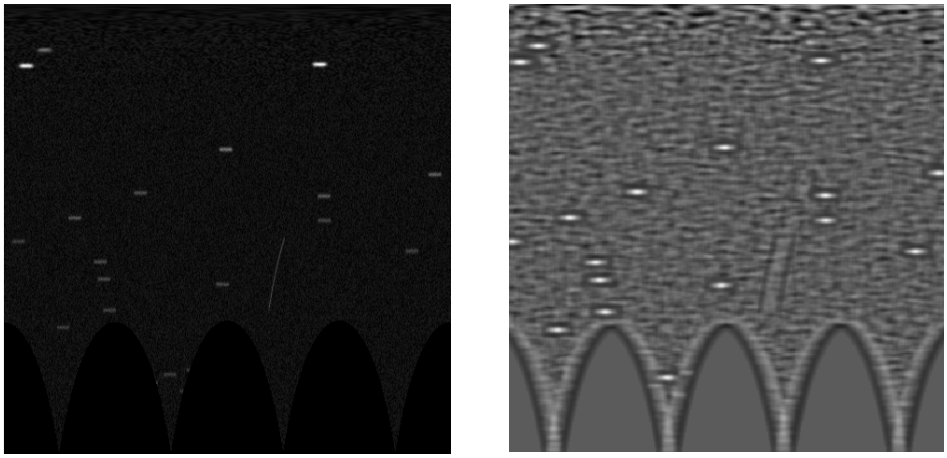

Figure 9 – (Left) Streaked star image re-sampled in polar coordinates. (Right) Match Filter result.

Choice of gridding parameters depends on the location of the center of rotation with respect to the image plane. The range of r and θ should be chosen such that the original image is completely sampled with as little out-of-bounds interpolation as possible. It is also worth noting that, in regions near the center of rotation, this re-sampling method produces artifacts from the image noise. This effect can be seen in the upper portion of figure 9. For small radii about the center of rotation the image is sampled too densely, leading to apparent correlations in the re-sampled image. This is typically only a problem when the center of rotation is within the boundaries of the image, however it can also arise in any case if the sampling density of (r, θ) is high.

The re-sampled image allows for additional analysis which is not possible in the original. For example, the apparent motion of the RSO is immediately apparent relative to the stellar background. Since all of the star streaks in the polar frame are straight with identical lengths, any streak which which deviates from this indicates some apparent motion. We can take an additional step in this direction by applying a matched filter to the re-sampled image. By estimating the streak length from the re-sampled image (or inferring it from an on-board gyro), we are able to create a template for any star in the field of view. Correlating this template with the image produces the result seen in right of figure 9. Note that we find a strong response for all star signals without the need for an adaptive matched filter.

6. GEODETICA: GENERALIZED SSA IMAGE ANALYSIS ENGINE

The Generalized Electro-Optical Detect Track ID and Characterize Application (GEODETICA) is a data reduction pipeline which combines advanced computer vision and image processing algorithms with online orbit determination and photometric analysis. The Matlab based software is available for testing and has been used to process simulated and real space object tracking datasets. In addition to the techniques presented in this paper, frame to frame association is performed using a Bayesian association method and Kalman filter for tracking of RSO and star positions as well as an online orbit determination approach which uses a particle filter based on the constrained admissible region. A key characteristic of the image processing pipeline is the use of multiple feedback

mechanisms between the image processing and the estimators supporting the orbit determination and characterization functions. Additionally, this software has been wrapped with the Astrometry.net star ID process which enables effective determination of key optical parameters, distortion, and inertial pointing for a wide array of ground and space based sensors.

7. CONCLUSIONS AND FUTURE WORK

This paper presented two key methods from computer vision used to determine interest points within imagery. The Harris Corner method was shown to provide a means to detect streak endpoints, but suffers from bias problems due to the smoothing necessary to localize the peaks. The method of Phase Congruency was shown to be quite promising in providing a means for direct space object segmentation and geometric analysis. Geometric inferences which can be made from extracted signals were discussed, including a method to evaluate the localization uncertainty of the extracted detections which is based on the computation of the Hessian of the detector response. Finally, a technique which exploits the additional information found in detected streak endpoints to provide a better centroid in the presence of curved star streaks is explained and additional applications for the presented techniques are discussed. By enabling the match filter in polar coordinates it is possible to distinguish very low SNR stars from RSO's in a single frame given that streaking motion is apparent over the exposure time. Future work will focus on the development and maturation of GEODETICA, an image processing pipeline developed at AFRL/RV which combines in a unique way, front end image processing with orbit determination and photometric analysis. It is the vision of the authors that this Matlab toolbox may be used to enable robust interpretation of imagery taken from ground and space sensors that are in various operating modes, and that the list of available options for sensor CON-OPS grows significantly by having a generalize framework which combines image processing with celestial mechanics and sensor attitude mechanics. The techniques presented here a just a few of the low-level processing algorithms which are used as building blocks to enable efficient interpretation of space object tracking data.

8. REFERENCES

1. Wallace, B., Rody, J., Scott, R., Pinkney, F., Levesque, M., and Buteau, S. "Toward and Array of Remotely Controlled, Autonomous Small Telescopes for Surveillance of Space." AMOS 2003, Kihei HI

2. Wallace, B. et. al. "The Near Earth Orbit Surveillance Satellite (NEOSSat)" AMOS 2004, Kihei HI

3. Harris, C. and Stephens, M., "A Combined Corner and Edge Detector," Proceedings of the 4th Alvey Vision Conference, Vol. 15, pp. 147-151.

4. Peter Kovesi, "Image Features From Phase Congruency". Videre: A Journal of Computer Vision Research. MIT Press. Volume 1, Number 3, Summer 1999.

5. Morrone, M., and Owens, R. "Feature Detection from Local Energy" Pattern Recognition Letters, 15:35-44, 1994

6. J. Crassidis and J. Junkins, Optimal Estimation of Dynamic Systems. CRC Press, 2nd ed., 2012.

7. G. Wahba. Problem 65-1: A least squares estimate of spacecraft attitude. SIAM Review, 7(3):409, July 1965.

8. [ESOQ2] D. Mortari. Second estimator of the optimal quaternion. Journal of Guidance, Control, and Dynamics, 23(5):885–888, 2000

9. D. Mortari, F. Markley, and P. Singla. An optimal linear attitude estimator. Journal of Guidance, Control, and Dynamics, 30(6):1619–1627, 2007.

10. Turin, George L. "An introduction to matched filters." *IRE Transactions on Information Theory* **6** (3) (June 1960): 311- 329